CMOS Torsional Micromirror

Eddie L.C. Ng and Kenneth T.Z. Oo
Department of Electrical Engineering and Computer Sciences
University of California, Berkeley
Email: eddieng@eecs.berkeley.edu, kenoo@eecs.berkeley.edu

Abstract

This paper presents the concept and design of a torsional micro-mirror system in a standard multi-metal layer CMOS process. The necessary torsional force is provided by CMOS comb drives that actuate in z-direction. Simulations yield that at least static $\pm 4^0$ rotation angle can be achieved with less than 50V for an arbitrary 3-metal-layer CMOS process with 0.5-μm layer thickness.

1. Introduction

Various torsional micromirrors have been studied and developed in silicon micromachining techniques. A typical MEMS torsional mirror is driven electro-statically by the electrodes buried in the substrate directly underneath the mirror. Magnetically driven torsional micro-mirror has also been demonstrated [1]. However, direct integration of these MEMS structures with electronics is desirable for systems with arrayed micromirrors and microsensors on a single monolithic chip. 100%-CMOS-compatible micromirrors will lower manufacturing costs and enable monolithic fabrication on typical CMOS chips. On-chip electronics also removes the interconnect bottleneck since active devices can be placed close to the microstructures.

A compelling example of this revolutionary CMOS-compatible micromirror technology would be the Digital Micromirror Device (DMD) invented in 1987 by Larry J. Hornbeck at Texas Instruments [2],[3]. DMD is a spatial light modulator in which an active micromirror is built on top of a CMOS SRAM cell. Electrostatic forces based on the data in the memory cell tilt the mirror either ±10 degrees to act as an ON and OFF switch for modulating the incident light. Although the DMD is fabricated by CMOS-like processes over a CMOS memory, the required fabrication steps are relatively complex and not readily available to general users [4].

Unlike the DMD in the TI's CMOS-like processes, the torsional micromirror investigated in this paper can be fabricated using more conventional multi-metal layer CMOS processing followed by a sequence of simple maskless dry-etching steps. The CMOS-MEMS process developed at Carnegie Mellon University is a maskless, post-CMOS micromachining in which the etching masks are provided by the interconnect metal layers in the standard CMOS process [5].

Taking advantage of the multi conducting layers readily available in CMOS processes, we propose a purely CMOS torsional micromirror. The mirror is electrostatically driven by the z-axis comb-finger actuators. In this paper, the post-CMOS micro-machining is briefly described first, followed by the principle of z-axis comb-finger actuation. Design issues and tradeoffs are discussed and simulation results are analyzed. Several test structures are proposed to verify the expected results.

2. Fabrication and Process Flow

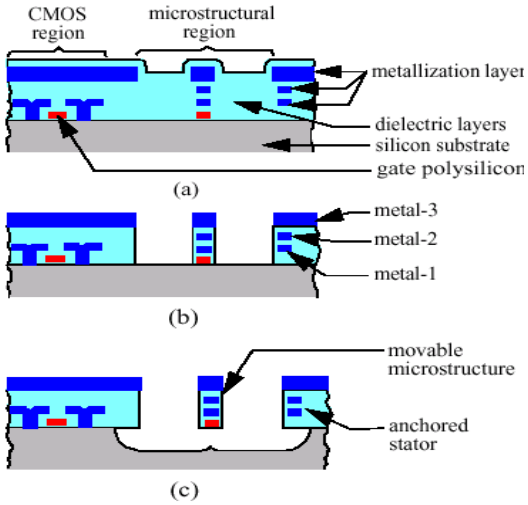

Figure 1. *Cross sections of device in each stage of the process flow.*
(a) Device from CMOS processing.
(b) After anisotropic isolation layers etch.
(c) After isotropic Si etch to release the mechanical structure.

The process flow is shown in Figure 1 to illustrate how our micromirror and comb drives can be fabricated using conventional CMOS processes. A thick top metal layer is used as the mask during the post-CMOS anisotropic CHF_3/O_2 Reactive Ion

Etch (RIE), which has a high selectivity of dielectric to metal, to define the microstructures [5]. This step etches oxide under the contact holes all the way down to the substrate, allowing the use of a dry SF_6/O_2 [5] or XeF_2 plasma etch [6] for the next step that isotropically undercuts the SCS substrate and releases MEMS structures.

This technique clearly has advantages. First, post-CMOS process is maskless. Second, the fact that dry etches are employed avoids the problem of potential adhesion of MEMS structures to the substrate. And lastly, the embedded multiple conducting layers in the structure enable electrostatic actuation in all x, y, and z axes [7],[8]. A simple Cadence layout of our micro-mirror is shown below in Figure 2.

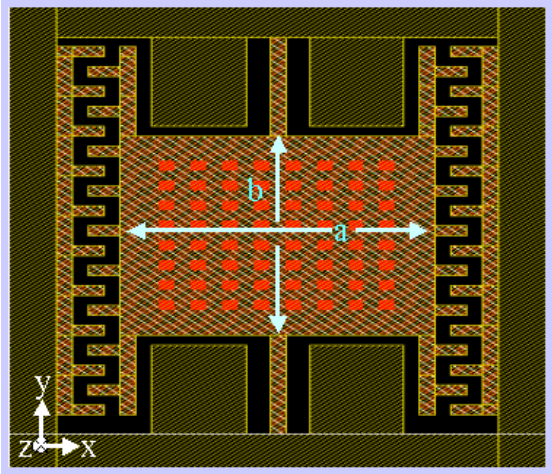

Figure 2: Simple Cadence layout of the micromirror in a 3-metal layer process. Note the use of vias to connect metal layers within the mirror while stator electrical layers are isolated electrically.

3. Design Theories

The basic concept of how z-axis actuation can be realized is depicted in Figure 3(a) and 3(b). One can start with the biasing configuration of the conducting layers as shown in Figure 3(a). All metal layers on the moving fingers are electrically connected to ground while all metal layers on the stators are separately biased. The CMOS comb drive in this configuration is equivalent to a conventional lateral-axis polysilicon comb drive.

When the bias voltage is removed from the metal-1 layer on the stators on one end of the mirror, a change in sidewall capacitance between the fingers occurs. This change in capacitance leads to an upward actuation of movable mirror fingers in z-direction and consequently the torsional rotation of the mirror itself. We also switch the bias and ground the metal-3 layer on the stators on the other end of the mirror to produce downward motion at the same time to double the torque.

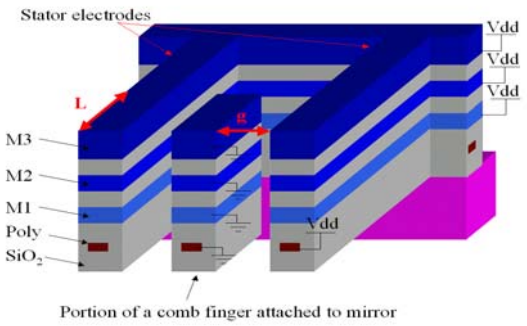

Figure 3(a): Close 3-D view of the comb drive actuators located on each side of the mirror.

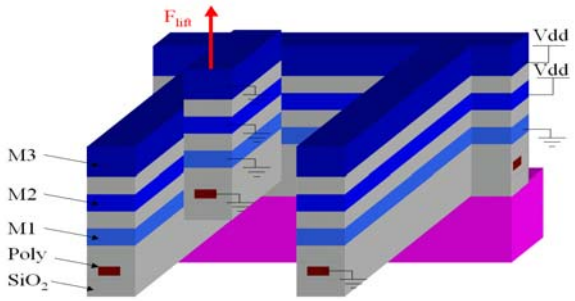

Figure 3(b): Electrode voltage scheme which provides vertical lifting force to rotate the mirror.

However, evaluating the change in sidewall capacitance with respect to z-displacement of the fingers is a nontrivial task. We hence used FastCap [9], a finite boundary element solver developed at M.I.T. to calculate 3-dimensional self and mutual capacitances of conductor surfaces. Model used for FastCap simulation is depicted in Figure 4 and results are shown and discussed in the later section.

Knowing $\frac{dC}{dz}$, the vertical electrostatic force that is acting on each end of the mirror is given by

$$F_{ez} = \frac{1}{2} N_g \left(\frac{dC}{dz} \right)_z V^2 \qquad (1)$$

where N_g is the number of comb-finger gaps and V the applied voltage. Assuming forces with the same magnitudes but in opposite directions on each end of the mirror (which will not be the case for the metal layers with different thickness), the resulting moment of the mirror about its support beam is

$$M_e = 2F_{ez}\left(\frac{a}{2}\right) = F_{ez}a \qquad (2)$$

where a is the length of the mirror side that is normal to the axis of rotation. The elastic recovery torque M_r of the torsion beams (with width w, length l, and thickness t) is

$$M_r = k_\theta \theta = \left(\frac{2\beta G w t^3}{3l} \right) \theta \qquad (3)$$

where k_θ denotes the torsional spring constant of the torsion support beams, β the correction factor, θ the mechanical deflection angle, and G the shear modulus of elasticity in N/m^2. Applying force balance concept, the voltage required for angular displacement of θ is

$$V(\theta) = \sqrt{\frac{\theta_{rad} k_\theta}{\frac{1}{2} N_g a \left(\frac{dC}{dz}\right)_{\frac{1}{2} a \sin\theta}}} \qquad (4)$$

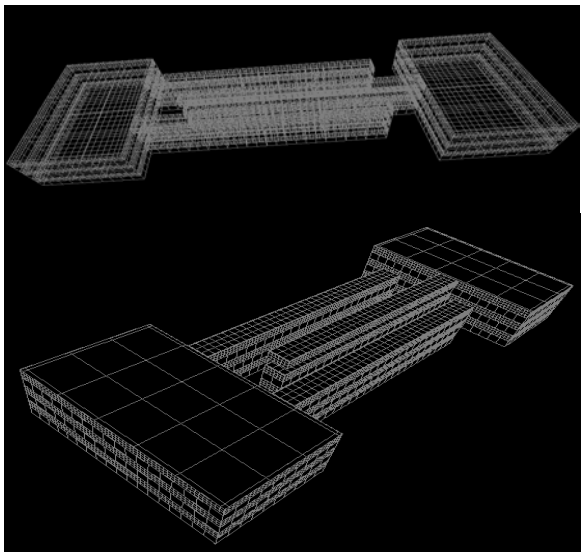

Figure 4: FastCap model of comb-finger pair with three metal layers for capacitance extraction.

4. Design Consideration

Driving the mirror from both ends has several advantages. First, it doubles the torque acting on the side of the mirror and hence allows a more compact design. Second, it minimizes the undesired vertical movement of the mirror and the support beam in z-direction. For a rigid mirror body, all vertical torque applied to the edge of the mirror will be fully translated into an angular displacement of the mirror about its axis of rotation, instead of a vertical shift or torsional bending of the mirror. The symmetry also reduces the lateral movement of the structure and eliminates the need for a laterally stiff support beam.

However, there are unfavorable effects that can arise in our system. For example, the top metal layer in most of the CMOS processes is much thicker than, say, the metal-1 layer. This unequal thickness of different conductor layers breaks up the symmetry once the mirror is actuated.

Another concern roots in the lateral curling of the microstructures. The difference in thermal expansion coefficients of metal and dielectric material creates vertical residual stress, making microstructures to curl out of plane. This undesirable effect could be resolved by process procedure which is usually not under a designer's control. Therefore, to combat this effect in a design prospective, careful study of lamination should be conducted. Experiments [10] have shown that the least delamination is observed when the maximum number of layers are included in the structures (see Table 1). Clearly, to obtain minimum delamination and maximum rigidity, mirror body and comb fingers are constructed with all available layers although this would impact the resonant frequency in a negative way due to bigger mass.

On the other hand, since the compliance of the torsion support beam is the most sensitive to its thickness (k_θ α t^3), the beam is constructed on a single metal layer. Ideally, the beam should also be long and narrow to yield better compliance and to reduce required voltage.

Laminate type	Nominal value
Metal 1	0.27 mm
Metal 2	1.3 mm
Metal 3	2.1 mm
Metal 1 + Metal 2	5.8 mm
Metal 1 + Metal 3	3.4 mm
Metal 2 + Metal 3	2.3 mm
M1 + M2 + M3	7.7 mm

Table 1: Radius of curvature of a 9μm-wide beam in a 3-metal layer CMOS process [10]

5. Test Structures

Mirror body	M3+M2+M1 and M1 only				
a,b	25μm	20μm	15μm	10μm	5μm
N_g	10,50,100				
L	5μm,10μm,15μm				
l	10μm, 15μm, 20μm				

Table 2. Geometries of the test structures

Table 2 summarizes an array of test structures suitable to experimentally study this mirror design. The parameters *a* and *b* are the length and width of the mirror, N_g is the number of gaps, *L* is the overlap of comb fingers and *l* is the length of the torsion support beam. The width of the torsion beam is the minimum feature size. Each structure has five bonding pads—one for the mirror, and four for the stators—to allow electrical connection needed for the conductor layers. Applied voltage will be varied from 5V to 100V to measure dc-deflection of the mirror. However, not all 432 different geometries on the test chip may be testable. Frequency response and z-displacement of mirror comb fingers can be measured on these test structures using a Michaelson optical interferometer system, and characterization of total static deflection as a function of voltage can be performed using simple optical setups.

These test structures would verify expected design operations as well as theoretical scaling proportionality. Tradeoffs between parameters can be studied from the experimental results as well.

6. Expected Results

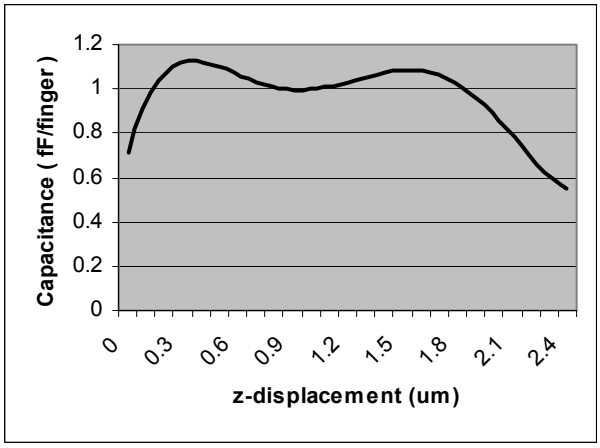

Figure 5: Capacitance vs. z-displacement for a comb-finger pair with engaged length of 10μm.

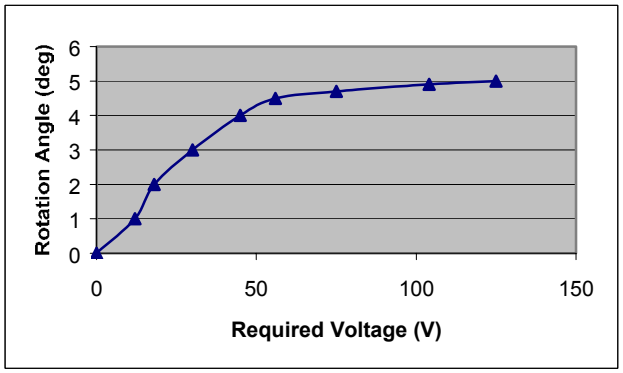

Figure 6: Rotation angle in degree vs. required voltage for $k_\theta = 0.5$ *nN-m/rad.*

Simulated capacitance versus z-axis displacement obtained from FastCap is shown in Fig. 5 for the case of grounded metal-1 and biased metal-2 and metal-3 on the stators. All three metal layers on the mirror fingers are grounded. All conductor and dielectric layers in our simulation model have 0.5μm-thickness.

Note that there are three extrema in Figure 5 where $\frac{dC}{dz}$ is zero. However, only the first critical point is valid as it marks the maximum z-displacement of the comb fingers for the biasing scheme. The electrostatic force between fingers saturates as the z-displacement approaches near the first peak ($z \approx 0.45\mu m$) and becomes independent of the applied voltage, as can be seen in Figure 6. Hence, an external force by other mean is required to go pass that critical point. Alternatively, one can remove the bias voltage from both metal-2 and metal-1 to obtain larger z-displacement. Various combinations of dielectric and metal layers with different thickness will also yield different maximum z-displacement and deflection angle.

The experimental results are expected to vary from our theoretically proposed values. The ends of the comb fingers and suspension beams may curl up out of plane or curl out in plane. Furthermore, released structures will have vertical mismatch and the top-metal layer which is used as a mask layer may be over-etched. Results may also vary from process to process. Nonetheless, experimental results should provide valuable insights for future development of the structure.

7. Conclusion

This paper has discussed how z-axis actuation can be realized in CMOS multi-metal-layer comb-drives and how torsional micromirrors can be made in a conventional CMOS process. Static dc-deflection of the mirror has been predicted using simulation and theories. The proposed test structures will be fabricated using the HP 3-metal 0.5μm n-well CMOS process available through MOSIS foundry. Availability of other CMOS fabrication processes and integration of sensing and feedback-control circuitry encourage further study and experimental verification on our proposed torsional micromirror structure.

References

[1] J.W. Judy, R.S. Muller, "Magnetic micro-actuation of torsional polysilicon structures," *Sensors and Actuators A*, 53 (1996) p. 392-397.

[2] L.J. Hornbeck, "Deformable-mirror spatial light modulators," *Proceedings of SPIE*, vol. 1150, Aug. 1989, p. 86-102.

[3] J. Younse, "Mirrors on a chip," *IEEE Spectrum*, vol. 30, no. 11, Nov. 1993, p. 27-31.

[4] M.E. Motamedi, M.C. Wu, K.S.J. Pister, "Micro-opto-electro-mechanical devices and on-chip optical processing," *Optical Engineering SPIE*, vol.36 no.5, May 1997, p. 1282-1297.

[5] G.K. Fedder *et al.*, "Laminated high-aspect-ratio micro-structures in a conventional CMOS process," *Sensors and Actuators A*, vol.A57, p.103-110.

[6] K.S.J. Pister *et al.*, "Controlled pulse-etching with Xenon Difluoride," *Transducers '97 International Conference on Solid-State Sensors and Actuators*, Chicago, June 1997, p. 665-668.

[7] H. Xie, G.K. Fedder, "A CMOS-MEMS lateral-axis gyroscope," *Technical Digest of the 14th IEEE International Conference on MEMS*, Switzerland, 21-25 January 2001, p. 162-165.

[8] H. Xie, G.K. Fedder, "Vertical comb-finger capacitive actuation and sensing for CMOS-MEMS," *Sensors and Actuators A*, 3127 (2001) p. 1-10 (paper in press).

[9] FastCap, Version 1.0, Research Laboratory of Electronics, MIT.

[10] D.F. Guillou, S. Santhanam, L. Carley, "Laminated Sacrificial-Poly MEMS Technology in Standard CMOS," *Sensors and Actuators A*, vol. A85, no.1-3, p. 346-355.